IJIE

INTERNATIONAL JOURNAL OF INTEGRATED ENGINEERING
ISSN: 2229-838X e-ISSN: 2600-7916

Vol. 18 No. 3 (2026) 210-226
https://publisher.uthm.edu.my/ojs/index.php/ijie

Carboxylated Adsorbent from Confiscated Cigarette Tobacco for Methylene Blue Removal

Saiful Azhar Saad[1]*, Khairudin Md Isa[1,2], Subash Candra Bose Gopinath[1,3], Farizul Hafiz Kasim[1,2] Naimah Ibrahim[4], Mohd Aizudin Abd Aziz[5]

[1] *Faculty of Chemical Engineering & Technology, Universiti Malaysia Perlis (UniMAP), 02600 Arau, Perlis, MALAYSIA*
[2] *Centre of Excellence for Biomass Utilisation, Universiti Malaysia Perlis, 02600 Arau, Perlis, MALAYSIA*
[3] *Institute of Nano Electronic Engineering, Universiti Malaysia Perlis (UniMAP), 01000 Kangar, Perlis, MALAYSIA*
[4] *Faculty of Civil Engineering & Technology, Universiti Malaysia Perlis (UniMAP), 02600 Arau, Perlis, MALAYSIA*
[5] *Faculty of Chemical and Natural Resources Engineering, Universiti Malaysia Pahang Al-Sultan Abdullah (UMPSA), 26300 Kuantan, Pahang, MALAYSIA*

*Corresponding Author: saifulazhar@unimap.edu.my
DOI: https://doi.org/10.30880/ijie.2026.18.03.014

Article Info

Received: 19 May 2025
Accepted: 18 November 2025
Available online: 30 April 2026

Keywords

Adsorption, dyes removal, confiscated cigarettes, chemical activation

Abstract

The widespread use of synthetic dyes in various industries has led to severe water pollution due to their toxic, mutagenic, and carcinogenic properties. This study investigates the potential application of an adsorbent prepared from confiscated cigarette tobacco for methylene blue (MB) removal. The adsorption performance of chemically treated confiscated cigarettes (CCC) was compared with untreated confiscated cigarettes (CC) and commercial activated carbon (CAC). The effects of contact time, initial MB concentration, adsorbent dosage, and solution pH on the MB removal efficiency were evaluated. SEM analysis of CCC revealed an increased in pore formation and structural modification, while FTIR confirmed the presence of carboxyl functional groups, indicating successful chemical activation. The optimum conditions for MB removal were 180 minutes of contact time, pH 8, with the adsorption capacity of 8.38 mg/g. Isotherm analysis showed that MB removal followed the Langmuir model (R^2 = 0.9734), indicating monolayer coverage, while kinetic data fitted the pseudo-second-order model (R^2 = 0.9861), suggesting chemisorption as the dominant mechanism involving strong adsorbate–adsorbent interactions and improved adsorption stability. CCC exhibited higher adsorption efficiency than CC, although CAC remained superior. This study introduces a novel waste management approach for the increasing quantities of confiscated cigarette waste generated due to stringent anti-smuggling enforcement. Overall, CCC demonstrates promising potential and economic feasibility as an alternative adsorbent, particularly for small-scale wastewater treatment applications.

1. Introduction

Rapid urbanization and industrialization have disrupted existing water resources. This is due to the increased pollution and inefficient water treatment systems. This scenario has contributed to an increasing demand for fresh water [1]. Industrial wastewater primarily consists of organic and inorganic substances, as well as highly toxic and hazardous substances such as dyes and heavy metals. Dyes are extensively utilized to impart color to a wide range of materials. The annual worldwide production of synthetic dyes is approximately 7×10^5 tons. There are over 10,000 types of known dyes and pigments [2], [3]. The textile industry is considered as the major contributor to water pollution, contributing about 20%, as reported by the World Bank Report [4]. Apart from textiles, dyes are widely used in various sectors, namely printing, pharmaceuticals, food, cosmetics, plastics, and paper. As a result, massive amounts of polluted wastewater have been produced, destroying aquatic ecosystems and polluting the water supply. The toxic, carcinogenic, and mutagenic effects of dyes were attributed by their molecular structures [5].

Dyes have been known for their detrimental effects on the ecosystem, human health, and the environment. Lellis *et al.* [5] reviewed the effects of dye contamination from textile industries in detail. To address this, several treatment methods have been proposed [6]. These methods include the coagulation-flocculation, oxidation, membrane separation, ion exchange, photochemical treatment, biological processes, and adsorption [7]. The advantages and limitations of these methods were compared in Table 1. Although these methods showed a high efficiency, they are often associated with high costs, require a large amount of energy, and produce sludge as byproducts. Table 2 provides a summary of prior studies on the removal of methylene blue (MB) using these methods. The limitations as outlined in Table 1 underscore the need for more cost-effective alternatives for dye removal [8]. Among various physicochemical treatment methods, adsorption is one of the preferred and most utilized method. Adsorption is governed by mass transport. This process involves the movement of a substance from the liquid phase to the solid's surface, where it adheres through physical and/or chemical interactions. Since its first introduction for dye removal, activated carbon has gained popularity and is commonly used as an adsorbent in wastewater treatment.

Commercial activated carbon (CAC) is commonly produced from coal, coconut shells, lignite, or wood. Its high surface area and well-developed porosity make it a standard benchmark material in adsorption studies. Generally, there are two types of activation methods: chemical and physical. In physical activation, high temperatures and longer activation times are required compared to chemical activation. However, in chemical activation, thorough washing is necessary due to the use of chemical agents. The activation process enhanced the pores' opening and enlarged existing pores, resulting in a net increase in surface area. Previous studies have frequently employed CAC for dye removal, as seen in the work of Dehmani *et al.* [9] for methyl orange adsorption and Kannan & Sundaram [10], who compared CAC with other bio-based adsorbents for MB removal. Rafatullah *et al.* [11] published a review paper on the effectiveness of CAC in MB removal.

Table 1 *Current treatment technologies for dye removal* [12]

Technology	Advantages	Limitations
Coagulation/flocculation	Cost-effective, straightforward method.	Significant amount of sludge production, large particle formation led to waste management challenges.
Advanced Oxidation Process	Swift and effective treatment process	High energy consumption, chemical dependency, by-product generation, and limited half-life.
Membrane separation	Capable of eliminating various types of dyes with high-quality treated effluent.	High cost due to high-pressure requirements, limitation in handling high volume, and thick sludge production.
Ion exchange	Suitable for a wide variety of dyes, and possibility for regeneration.	Expensive due to the requirement for absorbent regeneration and/or disposal. Less efficient for dispersing dyes.
Photochemical	No sludge formation, minimal chemical usage, and effective for treating recalcitrant dye.	Costly, by-product generation, technical limitation.
Biological treatment method	Effective for removal of certain dyes.	Technology is in the development stages and not yet commercialized.
Adsorption	Cost-effective and widely accepted method	Involved slow processes, requirement of optimal environment, and demand for maintenance and nutrition supply.

Int. Journal of Integrated Engineering Vol. 18 No. 3 (2026) p. 210-226

Table 2 *Reported studies on* methylene blue (*MB) removal using different technologies*

Technology	Summary	MB Removal Efficiency	Reference
Coagulation/flocculation	Biomaterials derived from bentonite and Opuntia Ficus Indica were used as substitutes for conventional coagulants and flocculants.	98.99%	[13]
	Lignin extracted from palm petiole waste was utilized for treating various types of pollutants	98.26%	[14]
Advanced Oxidation Process	A Fenton-like system was assessed for its ability for MB adsorption and degradation by utilization of Fe^{2+} ion sources from iron oxide nanoparticles	100%	[15]
	This study focused on optimizing operational parameters for methylene blue removal through persulfate oxidation, using SPS as an oxidant.	-	[16]
Membrane Separation	The removal of MB was conducted by employing (PSF/TiO_2) composite membrane, which undergoes UV-activated superwetting ability	90.8	[17]
	The MB removal study was conducted by utilizing chitosan/adipic acid cross-linked membrane (CS/AA).	100%	[18]
Ion exchange	In this study, the ion exchange methods were used to create iron/bentonite composite for photocatalytic degradation of MB.	100%	[19]
	Clinoptilolite samples ion-exchanged with zinc chloride at varying concentrations of clinoptilolite and zinc chloride prepared using solid phase ion-exchange method were used.	95.4%	[20]

Although it is widely used, the cost of activated carbon remains one of the significant drawbacks [21]. Furthermore, complexing agents are required to enhance their effectiveness in removing inorganic substances. Consequently, its high cost and limited efficiency hindered its widespread applications, especially for small-scale industries. Recently, there has been a growing emphasis on researching alternative adsorbents to replace costly activated carbon. Attention has shifted toward adsorbents with high binding capacities that can effectively remove dyes from contaminated water at lower costs. Natural materials that are abundantly available, as well as industrial by-products or agricultural biomass, hold promise as inexpensive adsorbents [22]. Given their low cost, these materials are often disposed of without undergoing regeneration once exhausted. Generally, adsorbents are considered low-cost if they require minimal processing, are widely available sources, or are generated as waste or by-products from other industries [23].

Malaysia's strong stance against cigarette consumption, through the implementation of various strategies, such as an increase in tax on tobacco products, has led to significant challenges, such as smuggling and illegal trade of cigarettes. Recent reports indicate that Malaysia has one of the highest rates of illicit cigarette trade globally, with confiscation amounting to billions of sticks annually [24]. The growing number of confiscated cigarettes presents an opportunity to reuse them to address issues such as wastewater treatment. Current disposal methods for confiscated cigarettes, including landfilling and incineration, lead to health hazards through water supply contamination and air pollution. Ahmad & Hamid [25] published an extensive review on the applications of cellulose-based material in raw tobacco for aquatic pollution remediation.

However, limited studies have reported on the use of confiscated cigarette tobacco as an adsorbent, despite its high carbon and cellulose content [26]. Furthermore, the introduction of carboxyl functional groups through citric acid activation, which may enhance MB uptake, has not yet been explored. Elio *et al.* [27] published their findings on lead removal using confiscated cigarettes that were pre-treated with NaOH and $ZnCl_2$. Their study

found that the adsorption capacity of chemically treated confiscated cigarettes using $ZnCl_2$ has improved, increasing from 56.818 to 84.746 mg/g, as compared to raw confiscated cigarettes.

In this study, we utilized citric acid as a chemical activation agent for tobacco in confiscated cigarettes to enhance the carboxylic acid content. Surface morphology and functional group analysis of untreated confiscated cigarettes (CC) and citric acid-treated confiscated cigarettes (CCC) were examined using a scanning electron microscope (SEM) and Fourier transform infrared spectroscopy (FTIR). Evaluating MB removal performance under various operational conditions is crucial for designing an effective adsorption system. Therefore, the effects of contact time, initial MB concentration, solution pH, and adsorbent dosage on the removal of MB were systematically studied. To further understand the adsorption mechanism, the equilibrium data were interpreted using the Langmuir and the Freundlich isotherm models. At the same time, the kinetic behavior was assessed using pseudo-first-order and pseudo-second-order models. The Weber-Morris intraparticle diffusion model was also applied to determine whether diffusion was the rate-limiting step. This study proposes a practical waste management strategy by converting confiscated cigarette tobacco into a low-cost adsorbent. The results highlight the environmental and economic advantages of this approach for sustainable, small-scale wastewater treatment applications.

2. Materials and Methods

2.1 Adsorbents Preparation

Commercial activated carbon (CAC) (Merck, Germany; analytical grade; particle size 100–200 mesh) was used as a reference sorbent for comparison with untreated confiscated cigarettes (CC) and chemically treated confiscated cigarettes (CCC). The CAC was acquired locally and used directly without modification. The specifications provided by the manufacturer are as follows: moisture 8%, pH value 5–6, loss on drying 15%, and ash 5%. Confiscated cigarettes were obtained from the Royal Malaysian Customs Department, Perlis Branch. Tobacco was separated from its wrapping and butts. Subsequently, the impurities, such as dust and paper residue, were removed by rinsing with distilled water. Following this, the tobacco was dried in an oven at 50°C for 24 hours. After that, the material underwent grinding and sieving to achieve a particle size of 200–250 µm. The materials were kept in closed containers until further use.

2.2 Citric Acid-Treated Confiscated Cigarettes

A mixture of 10 g of tobacco and 50 mL of citric acid (0.5 M) was heated in a muffle furnace at 300°C. The mixture was then rinsed with distilled water to adjust the pH of the resulting sample to 7. Subsequently, the mixture was soaked in a 2% sodium bicarbonate solution for 24 h to eliminate excess acid. The mixture was rewashed with distilled water to remove any residual sodium bicarbonate. After being dried in the oven for 24 h at a temperature of 50°C, the CCC was ground and sieved to obtain particles with a size of 200–250 µm. Lastly, the CCC samples were stored in a container until further use**.**

2.3 Methylene Blue (MB) Preparation

The methylene blue (MB) dye (analytical grade, Sigma-Aldrich) used in this study was obtained from a local supplier. For 1000 mg/L of MB stock solution, an accurate weight of MB dye was dissolved in deionized water. Successive dilution was performed to achieve the desired concentrations (Fig. 1). An ultraviolet-visible spectrophotometer (Hitachi, Model U-2910) was employed to measure the absorbance at 664 nm to determine the concentration of MB both before and after treatment. The instrument calibration was linear in the range of 1-100 mg/L (R^2 = 0.999), and the samples exceeding this range were further diluted to ensure accurate measurement.

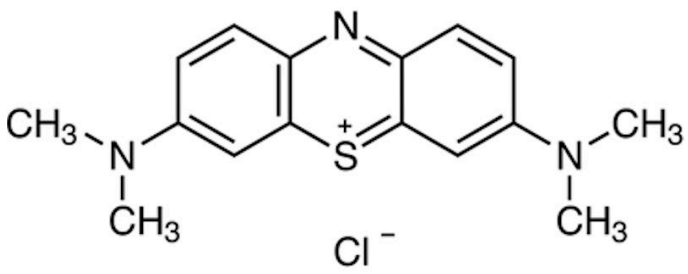

Fig. 1 *Structural formula of MB*

Int. Journal of Integrated Engineering Vol. 18 No. 3 (2026) p. 210-226

2.4 Adsorption Study

The batch adsorption experiments were carried out using a cylindrical batch-like contactor (5 cm inner diameter, 50 cm height, with a working volume of 750 mL), as illustrated in Fig. 2. In each run, 500 mL of MB solution was prepared at a predetermined initial concentration, pH, and adsorbent dosage. The mixture was agitated at 200 rpm and maintained at room temperature (26 ± 1 °C). To obtain the desired pH, 0.1 M NaOH or HCl was added to the MB solution. At the specific time intervals, the MB samples were withdrawn, and the supernatant was separated by centrifugation at 4500 rpm for 5 minutes. The supernatant was analyzed to determine the residual MB concentration. The experiments were conducted at various operating conditions at equilibrium, which include adsorbent dosages (0.2–1.0 g), initial MB concentrations (20–100 mg/L), and solution pH (2–12).

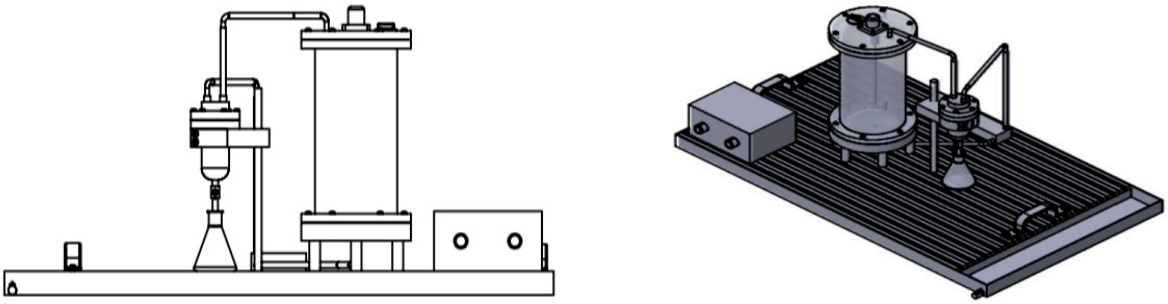

(a) **(b)**

Fig. 2 *Experimental setup for adsorption study (column diameter = 5 cm, column height = 50 cm, agitation speed = 200 rpm) (a) Front view; (b) 3D view*

The removal efficiency of MB and the adsorbent capacity were calculated using Eq. 1 and Eq. 2, respectively:

$$\% \text{ MB Removal} = \frac{C_i - C_o}{C_o} \times 100\% \quad (1)$$

$$Q_e = \left(\frac{C_o - C_e}{V}\right) m \quad (2)$$

2.5 Adsorption Isotherms

Adsorption isotherms describe the correlation between the adsorption capacity of CCC and the MB concentration at the equilibrium. In this study, the equilibrium experiment data were fitted to the adsorption isotherm models, namely the Langmuir and the Freundlich models. In adsorption studies, isotherms are useful in predicting the mechanisms of the adsorption process; thus, it is critical to have a proper understanding of adsorption isotherms to improve adsorption mechanism pathways and design effective adsorption systems. In this study, the adsorption isotherms were examined under optimum conditions (pH 6, contact time 180 min, and adsorbent dosage 1.0 g) by varying the initial methylene blue concentration from 20 to 100 mg/L.

The adsorption mechanism of MB onto the CCC was investigated utilizing two widely recognized isotherm models: the Langmuir and the Freundlich models. The Langmuir equation can be expressed as follows (Eq. 3):

$$\frac{1}{Q_e} = \frac{1}{Q_{max} K_L} \frac{1}{C_e} + \frac{1}{Q_{max}} \quad (3)$$

The constants Q_{max} and K_L can be determined by plotting $(1/Q_e)$ vs. $(1/Ce)$.

A non-linear adsorption model based on the Freundlich isotherm describes multilayer adsorption with a heterogeneous energy distribution across active sites and interactions with MB molecules. The Freundlich equation is as follows (Eq. 4):

$$Q_e = K_f C_e^{1/n} \quad (4)$$

Eq. (4) above can also be represented as a linearized equation as follows (Eq 5):

$$\log Q_e = \log K_f + \frac{1}{n}\log C_e \quad (5)$$

The values of K_f and n can be determined from the plot of log (Q_e) vs log (C_e).

2.6 Kinetic Study

A kinetic study is a commonly utilized method for assessing the rate and mechanism of MB removal. The pseudo-first (PFO) and second-order (PSO) are the most frequently employed kinetic models for these analyses. This study was conducted at varying contact times while keeping other parameters constant. The rate constant for the PFO can be determined by utilizing the first-order equation by Lagergren (Eq. 6):

$$\log(q_e - q) = \log(q_e - \frac{k_1 t}{2.303}) \quad (6)$$

where q_e and q represent the quantities of dye absorbed (mg g^{-1}) at equilibrium and at a specific time t (min), respectively, as defined by Eq. 2 and Eq. 7:

$$q_t = \frac{(C_o - C_t)W}{V} \quad (7)$$

where C_o and C_e represent the MB's initial and equilibrium concentrations (mg/L), respectively, V denotes the volume of the solution (L), and W indicates the mass of the adsorbent (g). C_t are MB concentrations at time t.

In addition to PFO and PSO models, which mainly describe surface reaction kinetics, adsorption can also be influenced by the rate of dye movement from the bulk solution into the pores of the adsorbent. To examine this behaviour, the Weber–Morris intraparticle diffusion model is often used. The model is written as (Eq. 8):

$$q_t = k_{id} t^{0.5} + C \quad (8)$$

where k_i represents the intraparticle diffusion rate constant, and *C* reflects the effect of boundary layer resistance. If the plot of q_t versus $t^{0.5}$ gives a straight line that passes through the origin, it suggests that intraparticle diffusion is the only rate-limiting step. However, if the line does not intersect the origin, it means that other mechanisms, such as film diffusion on the external surface, also control adsorption. In many adsorption systems, the plot exhibits more than one linear segment, typically representing different stages: rapid external diffusion at the beginning, followed by gradual diffusion into the pores, and finally a plateau as equilibrium is achieved. Therefore, applying the Weber–Morris model helps to clarify whether chemisorption alone controls the kinetics or whether diffusion resistance also plays a role.

2.7 Characterization of Prepared Adsorbents

The surface morphology of CC and CCC was visualized using an FEI Quanta 200 scanning electron microscope. The PerkinElmer Spectrum Two FTIR spectrometer was used to determine the spectra of the adsorbents for both prepared adsorbents, CC and CCC, within a wavelength range of 400-4500 cm^{-1}.

3. Result and Discussion

3.1 Effect of Contact Time

The effect of contact time on MB removal using CAC, CC, and CCC was investigated. To evaluate the effect of contact time on MB removal, the mixing time was varied from 15 to 210 minutes. In this experiment, other parameters such as adsorbent dosage (1.0 g), pH (6.0), and initial concentration (100 mg/L), were kept constant. For CAC, rapid removal of MB was achieved at the early stage of the process (0-30 minutes), and equilibrium was reached after 45 minutes. This is attributed to CAC's high surface area as well as a well-developed pore structure (Fig. 3).

Both CC and CCC exhibit a rapid adsorption rate during the initial stage of the adsorption process. For CCC, 20.4% and 39.7% of MB removal were recorded after 15 and 30 minutes. While the same pattern was observed for CC, it shows a slightly lower MB removal rate, with only 13.9% and 32.0% removal after 15 and 30 minutes, respectively.

Int. Journal of Integrated Engineering Vol. 18 No. 3 (2026) p. 210-226

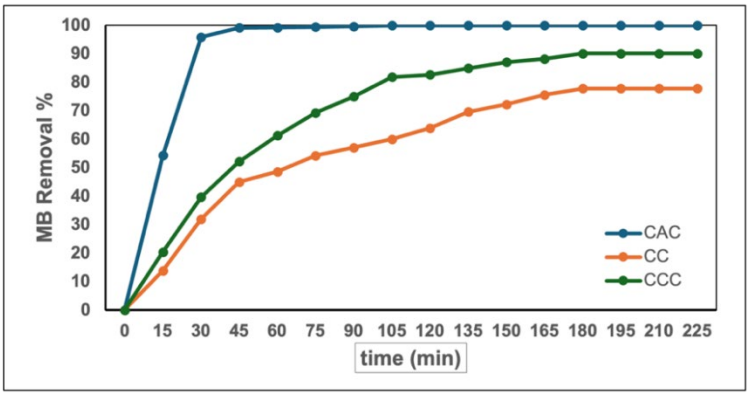

Fig. 3 *The effect of contact time on MB removal (adsorbent dosage = 1.0 g, pH = 6, initial concentration = 100 mg/L)*

The rapid MB removal by CC and CCC at the initial stage is due to the availability of active sites on the adsorbent surface. As the contact time increases, this site is gradually occupied, resulting in a decrease in the rate of MB removal. In addition, the reduction in the rate of MB removal at the later stages was due to several factors, including diffusion limitations and intraparticle resistance between adsorbed and free MB molecules [28]. The rate of MB removal by CC and CCC has become constant after 180 minutes, indicating the equilibrium has been reached. Thus, 180 minutes was used as an equilibrium time for the subsequent study. At the equilibrium, there's no further increase in the removal of MB due to the saturation of the active site of the adsorbents.

3.2 Adsorption Capacity for MB Removal

The adsorption capacity is the maximum amount of MB that is removed per unit mass of adsorbent. It is typically expressed in units of the adsorbate for unit mass of adsorbent (mg/g). This provides valuable insights into the degree of interaction between the adsorbent and adsorbate under specific conditions. This parameter provides more accurate information on adsorbent performance than removal efficiency, as adsorbent performance depends on the initial concentration and dosage. Table 3 compares the adsorption capacity in this study with reported findings in previous studies on MB removal.

Table 3 *Comparison of reported adsorption capacity*

Type of Adsorbent	Activation Procedure	Adsorption Capacity (mg/g)	Reference
Hazel nut shells	Dried hazel nut shells were mixed with $ZnCl_2$ (30% wt.), dehydrate at 103 C for 6-24 hr, and activated at 750-850 °C for 2 hr in the presence of N_2.	8.82	[29]
Coir pith	Dried coir pith powder (250-500 µm) was mixed with concentrated H_2SO_4 and heated in muffle furnace.	5.87	[30]
Coal fly ash	Coal fly ash was mixed with $ZnCl_2$ (30% wt.), dehydrate at 103 °C for 6-24 hr, and activated at 750-850 °C for 2 hr in the presence of N_2.	4.11	[29]
Walnut shell	The oven dried walnut shell was mixed with $ZnCl_2$ (30% wt.), dehydrate at 103 °C for 6-24 hr, and activated at 750-850 °C for 2 hr in the presence of N_2.	3.53	[29]
Fir wood	Dried fir wood was heated at a rate of 5 C/min from room temperature to 450 °C, in the presence of N_2. The char was then soaked in the concentrated NaOH solution, followed by oven dried.	1.21	[31]
Corncob	Corncob was used to prepared activated char in the presence of N_2. The chars were mixed with KOH and heated at 130 °C for 24 hr.	0.84	[32]
Confiscated cigarettes		8.48	*Current study*

Although few adsorbents, such as hazelnut shells and coir pith, have reported similar or slightly higher adsorption capacities, most of them were produced by using strong acids or alkaline solutions, including H_2SO_4, $ZnCl_2$, NaOH, or KOH, at high temperatures. These activation methods can create highly porous structures, which explains the superior uptake in some cases (e.g., hazelnut shells at 8.82 mg/g). However, they also generate acidic or alkaline waste that must be neutralized before disposal. In this study, CCC achieved an adsorption capacity of 8.48 mg/g, which is comparable to hazelnut shells and higher than several other waste-derived adsorbents, including coal fly ash, walnut shells, fir wood, and corncob (Table 3). The application of citric acid as an activation agent offers several advantages over other activation methods. The benefits include a reduction in the use of strong corrosive chemicals and the generation of toxic waste. The use of citric acid, a biodegradable material, is a more environmentally friendly process and a safer method for waste generation, presenting a more sustainable alternative in adsorbent development.

3.3 The Influence of Initial MB Concentration

Fig. 4 shows that the efficiency of MB removal by using CAC was not affected by the initial concentration, achieving almost complete removal (i.e., 100%) regardless of the initial dye concentration. The good adsorption performance of CAC was attributed to its high adsorption capacity and surface structure. Although high concentrations are typically associated with low efficiency, the CAC application is favorable due to its ability to completely remove pollutants at various concentrations [33]. In contrast, the removal of MB by CC and CCC decreased with the increase of initial MB concentration, despite the increasing amount of MB removed. At a high initial concentration, more active sites become saturated, resulting in a greater number of MB molecules competing for the limited active sites. Additionally, an increase in mass transfer resistance occurs at high initial concentrations, resulting in slow diffusion and consequently low MB removal.

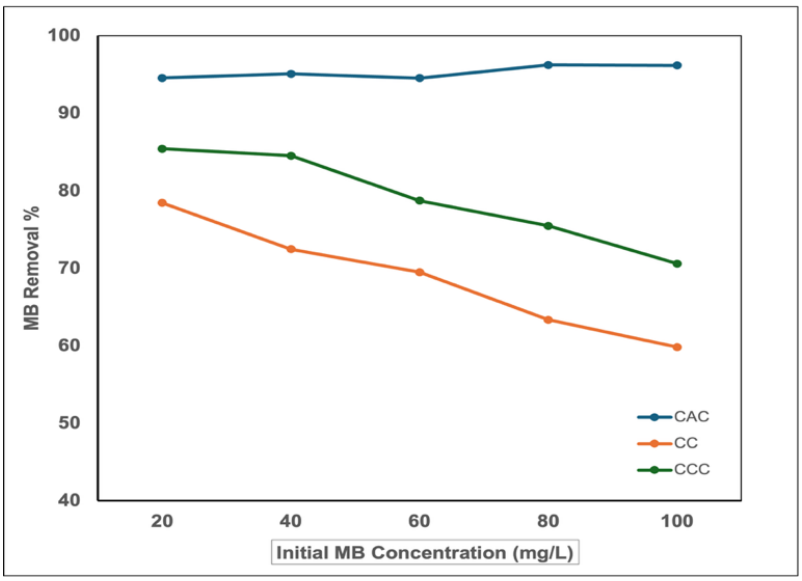

Fig. 4 *The effect of initial concentration on MB removal (adsorbent dosage = 1.0 g, pH = 6, contact time = 180 min)*

Comparing the performance of CC and CCC, while both adsorbents exhibit the same trend, it is worth noting that the reduction in removal efficiency of CCC is slightly lower than that of CC, from 85.4% to 70.6% when the initial concentration increases from 20 mg/L to 100 mg/L. For comparison, the MB removal by CC dropped from 78.44% to 59.82%. This is due to the more available active site on CCC with better surface morphology. The limited active site in CC also contributed to the aggregation of MB molecules, which hindered the MB molecules from reaching the adsorbent surface, thus further reducing its efficiency. The trend observed in this study aligns with the findings of other reported studies [34].

3.4 The Effect of pH

The effect of the solution's pH on the efficiency of MB removal using the prepared adsorbents is illustrated in Fig. 5. For CAC, the removal of MB was not significantly affected by pH variation, with nearly 100% removal at all pH levels studied. Although the pH can influence electrostatic interactions, the removal of MB using CAC typically involves a non-electrostatic interaction. These interactions encompass π-π stacking between the aromatic rings

Int. Journal of Integrated Engineering Vol. 18 No. 3 (2026) p. 210-226

of MB and the surfaces of CAC, as well as hydrogen bonding and hydrophobic interactions [34]. These interactions remain consistent across all pH variations, ensuring a consistently high removal of MB.

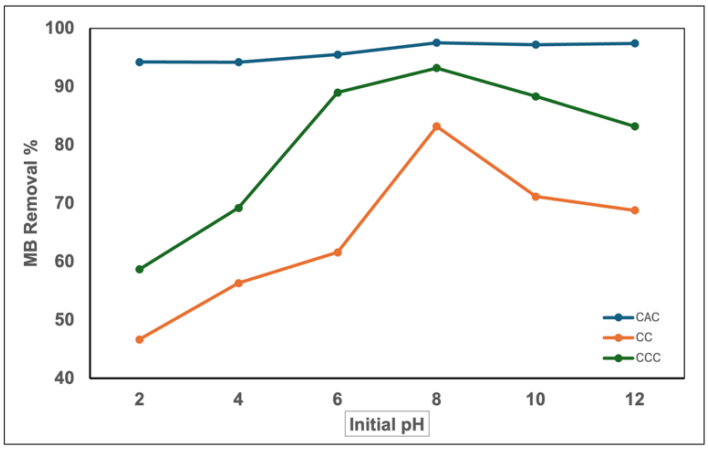

Fig. 5 *The effect of pH on MB Removal (contact time = 180 min, adsorbent dosage = 1.0 g, MB concentration = 100 mg/L)*

The pH variation influences the efficiency of MB removal by using CC and CCC, with both showing the highest efficiency at pH 8. In the acidic condition, the surface of CC and CCC became positively charged due to protonation [35]. As MB is cationic in nature, the electrostatic repulsion between the positive charge of the adsorbents and the MB molecules resulted in low removal efficiency. At a neutral pH (pH = 7), the surface charge of the adsorbent is reduced, thereby reducing the effects of electrostatic interactions during the removal process [36]. At this pH, other interactions, such as van der Waals forces and hydrogen bonds, influence the adsorption process, contributing to better performance in this condition compared to acidic conditions. In alkaline conditions, the surface of CC and CCC becomes negatively charged due to the deprotonation of its surface. This has created a strong electrostatic attraction between the adsorbent's surface and cationic MB molecules, thus enhancing the removal efficiency [34]. From Fig. 5, it was observed that the removal of MB by CC and CCC decreased at pH levels above 8. This is because, in the strong alkaline conditions, MB molecules need to compete with excess OH^- ions. This competition thus reduced the efficiency of MB removal [37].

3.5 The Influence of the Adsorbent Dosage

For CAC, the removal of MB from aqueous solution was not affected by the adsorbent dosage (Fig. 6). The removal efficiency was nearly 100% for all adsorbent dosages. This is attributed to the high adsorption capacity, large surface area, and well-developed pores in the CAC. Also, CAC possesses a high number of active sites, and its abundant functional groups provide strong van der Waals and electrostatic forces with the MB molecules. Due to the described surface morphology, CAC is highly efficient in MB, achieving almost complete removal even at low dosage.

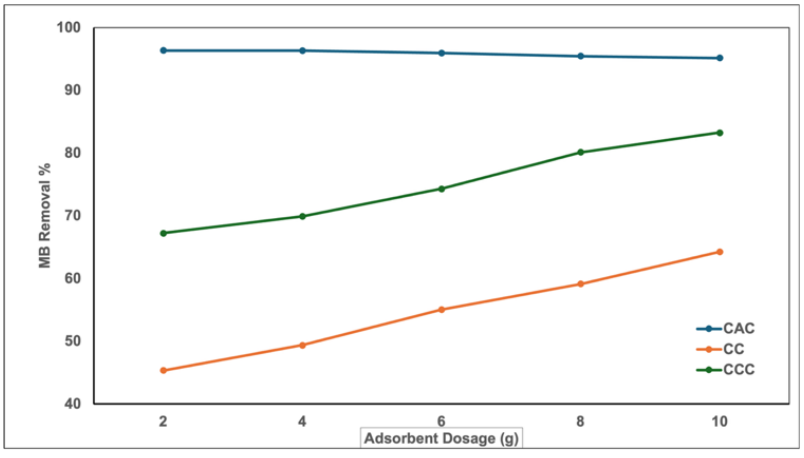

Fig. 6 *The effect of adsorbent dosage on MB removal (contact time = 180 min, pH = 6, initial MB concentration = 100 mg/L)*

In contrast, we found that the MB removal by using prepared adsorbents, CC and CCC, is affected by the adsorbent dosage. As the adsorbent dosage increased, the removal of MB also increased. This is due to the increase in the number of available active sites on both adsorbents, which indirectly reduces the competition among the MB molecules for the binding sites [17], [38]. For CC, the MB removal increased from 45.3% to 64.2% as the adsorbent dosage increased from 0.2 g to 1.0 g. CCC shows an increase in MB removal from 67.24% to 83.27% as the adsorbent dosage increases from 0.2 g to 1.0 g. A better performance by CCC compared to CC was due to the improved porous structure and increased number of active sites resulting from chemical activation [39].

Overall, the findings suggest that the adsorbent dosage plays an important role in the removal of MB. As the adsorbent dosage increased, more available active sites would reduce the competition between the MB molecules, thereby improving the efficiency of the adsorbents.

3.6 Surface Functional Group Analysis

The FTIR spectrum of all adsorbents, as shown in Fig. 7, revealed distinct functional groups from 3700 to 3000 cm^{-1}, indicating O-H stretching vibration. This O-H stretching vibration suggests the presence of hydroxyl groups on their surface [40].

In addition, a smaller peak in the region of 1500 to 1000 cm^{-1} was also observed for all adsorbents. This peak represents C-O stretching, confirming the presence of an aromatic ring, ether, phenol, or other oxygenated carbon structures [25]. The FTIR spectrum of CAC also shows smaller peaks in the 1700-1500 cm^{-1} range, which typically correspond to C=O stretching vibrations, indicating the presence of carbonyl groups, such as carboxylic acids or ketones. These functional groups contain an oxygen, which enhances the adsorbent's performance in removing polar molecules, such as MB. In the same region, a sharper peak was observed for CC. Below 1000 cm^{-1}, the observed features were attributed to the presence of inorganic impurities and the porous structure, which contributed to the effectiveness of CAC in MB removal [41].

In the region ranging from 3000 to 2800 cm^{-1}, a range of peaks was observed for both prepared adsorbents, CC and CCC. These peaks represent C-H stretching, indicating the presence of aliphatic hydrocarbons, which are commonly found in nicotine or tar residue [42]. The FTIR spectrum of CCC displayed a noticeable difference in the region, ranging from 1720 to 1735 cm^{-1}. A new, sharper peak indicates C=O stretching vibrations, which are associated with carboxylic acid. The result has confirmed the successful introduction of carboxyl (-COOH) groups through citric acid modification [43].

To summarize these observations, the main FTIR peak positions, functional groups, compound classes, and references for CC and CCC are listed in Table 4.

Table 4 *FTIR peak positions and functional group assignments for CC and CCC*

Adsorbent	Peak Position (cm^{-1})	Functional Group	Compound Class	Reference
CC	~3340	O–H stretching	Hydroxyl groups (cellulose, lignin, phenols)	[41]
	2920–2850	C–H stretching	Aliphatic $–CH_2/–CH_3$ (nicotine, tar residues)	[44]
	1700–1600	C=O stretching	Carbonyls (aldehydes, ketones, weak –COOH)	[42]
	1500–1000	C–O stretching + C=C	Cellulose, lignin, esters, ethers	[26]
CCC	~3340	O–H stretching	Hydroxyl + hydrogen-bonded –COOH groups	[43]
	2920–2850	C–H stretching	Aliphatic hydrocarbons	[45]
	1720–1735	C=O stretching	Carboxylic acids (–COOH) formed during citric acid activation	[43]
	1600–1510	Aromatic C=C	Lignin/aromatic rings	[45]
	1500–1000	C–O stretching	Alcohols, esters, phenols (increased after activation)	[26]

As shown in Table 4, both CC and CCC share typical lignocellulosic functional groups, including O–H, C–H, and C–O. However, the appearance of a distinct C=O peak at 1720–1735 cm^{-1} in CCC, which is absent in CC, provides strong evidence of carboxyl (–COOH) group formation due to citric acid activation. This modification increases the number of active sites capable of forming electrostatic interactions with cationic methylene blue molecules, thereby improving adsorption performance.

Int. Journal of Integrated Engineering Vol. 18 No. 3 (2026) p. 210-226

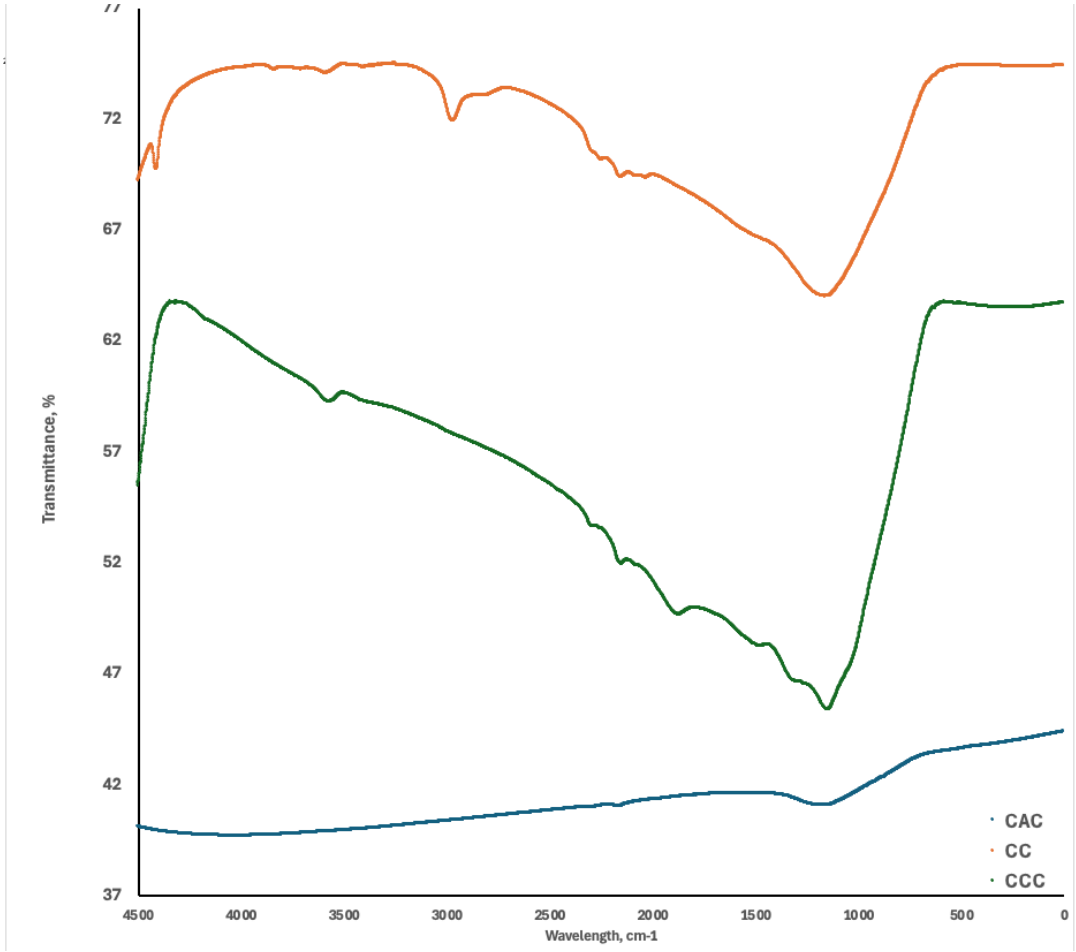

Fig. 7 *FTIR spectra for different types of adsorbents*

3.7 Surface Morphology by Scanning Electron Microscope

In this study, the surface morphology of the adsorbents was analyzed using an SEM instrument. The morphology was captured at 1,000× magnification. Fig. 8 depicts the SEM images for all the adsorbents used.

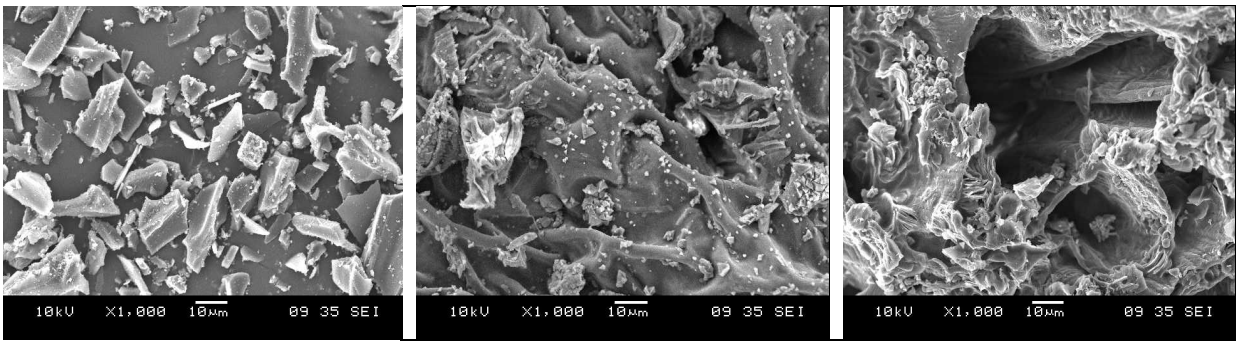

Fig. 8 *Scanning electron microscope images of (a) CAC, (b) CC, and (c) CCC at 1,000× magnification*

The SEM image of the CAC revealed smaller, but uniform particle sizes ranging from 5 to 50 µm. This contributed to its high surface-to-volume ratio. CAC also shows a homogeneous, well-developed, and evenly distributed pore structure [43]. The well-refined surface morphology of CAC contributed to its high efficiency in removing MB. For CC, the SEM image displayed irregular surface morphology with a layered structure. Scattered granular particles, which are commonly caused by incomplete carbonization, were also observed. The poor pore uniformity and surface homogeneity contributed to its lower efficiency, compared to CAC and CCC. Although CCC also displayed an irregular surface morphology, sharper edges and more fractured and angular structures were observed. This is likely formed during the chemical activation process [17]. This has contributed to the formation

of micropores and mesopores, thereby improving its surface area. Additionally, chemical activation has enhanced the porosity and surface roughness, providing more active sites for MB removal. The findings for the SEM image support the experimental results conducted in this study.

3.8 Adsorption Isotherms for MB Removal

Table 4 summarises the adsorption isotherm constants for MB removal on CCC based on the Langmuir and the Freundlich models. The experimental data from the adsorption study at the different initial MB concentrations were analyzed to evaluate the mechanism of MB removal using CCC. The experimental data were found to fit the Langmuir isotherm model better (R^2 = 0.9734) than the Freundlich model (R^2 = 0.6189). It suggests that MB removal on the CCC occurred on a monolayer and homogeneous adsorption site, with no interaction between MB molecules.

From the Langmuir isotherm plot (Fig. 9(a)), the Langmuir isotherm constant, K_L, of 0.1719 was obtained, indicating good adsorption with a strong affinity. The Q_{max} value was obtained from 1/slope and was determined to be 8.38 mg/g, which is slightly lower than the values reported in other studies using chemically activated adsorbents with H_3PO_4 and KOH [12], [27]. The calculated separation factor (R_L = 0.0036) between 0 and 1, and the Freundlich constant (n = 1.94) indicate that MB removal using CCC is favourable, particularly at higher concentrations. (Fig. 9(b)). Additionally, the K_F value indicated a relatively low adsorption capacity, which is consistent with the calculated value. Overall, the removal of MB by CCC can be better described using the Langmuir isotherm model, based on the higher correlation coefficient value (Table 5(a) & (b)).

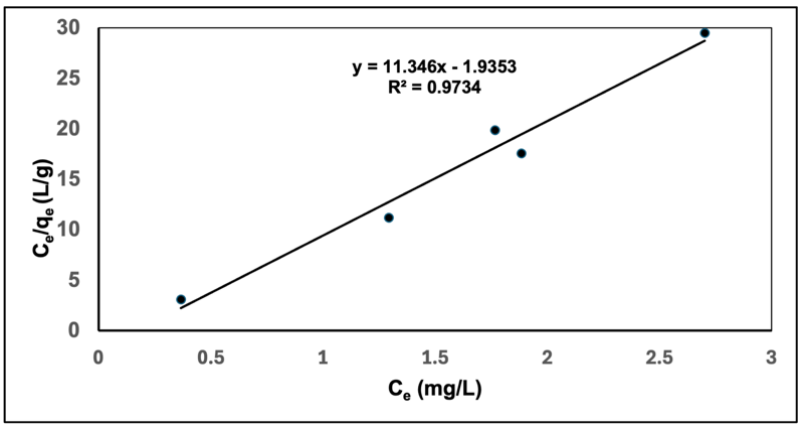

Fig. 9(a) *Data fitting with the Langmuir isotherms model*

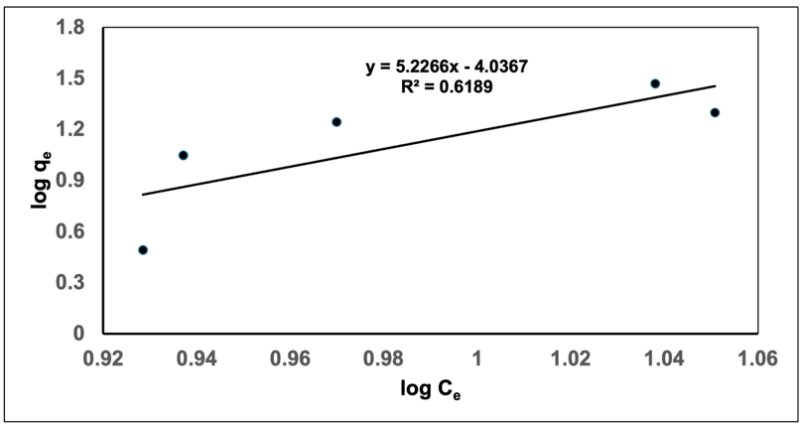

Fig. 9(b) *Data fitting with the Freundlich isotherms*

Table 5(a) *Langmuir isotherm parameters for MB removal by CCC*

Langmuir			
R^2	Q_{max}	K_L	R_L
0.9734	8.38	0.364	0.0036

Int. Journal of Integrated Engineering Vol. 18 No. 3 (2026) p. 210-226

Table 5(b) *Freundlich isotherm parameters for MB removal by CCC*

Freundlich			
R^2	n	1/n	K_f
0.6189	1.84	0.543	1.228

3.9 Adsorption kinetic study

The adsorption kinetics are important for understanding the rate and mechanism of MB removal by using CCC. The adsorption kinetics were evaluated using the pseudo-first-order (PFO) and pseudo-second-order (PSO) models to determine the mechanism and rate-controlling step of MB uptake by CCC. The corresponding kinetic parameters are summarised in Table 6, whilst the linearized plots of both models are presented in Fig. 10(a) and 10b.

Table 6 *Calculated values for PFO and PSO*

PFO			PSO	
Q_m	R_1^2	k_1	R_2^2	k_2
8.38	0.9611	0.9285	0.9861	0.0027

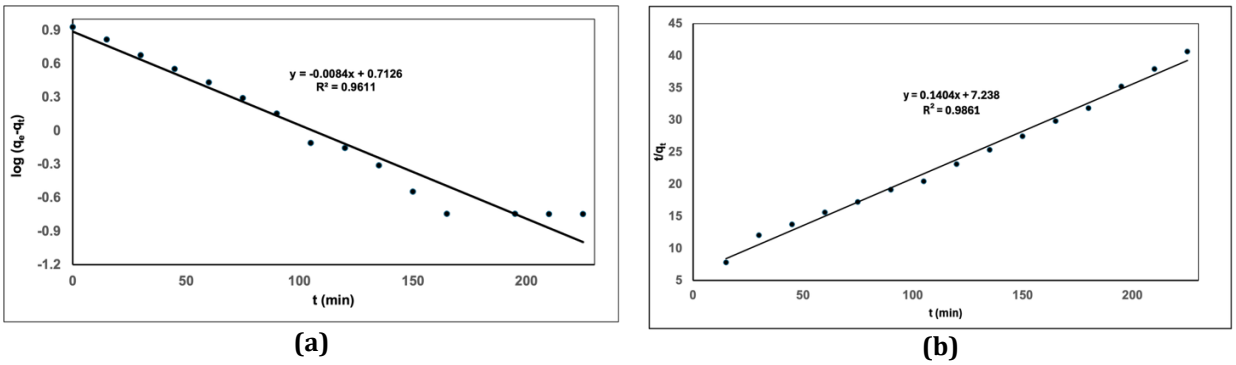

(a) **(b)**

Fig. 10 *Adsorption kinetics of MB removal by CCC (a) PFO; (b) PSO*

The PFO model (Fig. 10a) exhibits a moderate linear relationship with a correlation coefficient of R^2 = 0.9611 (Table 10(a)), suggesting that this model may not fully describe the adsorption mechanism of MB onto CCC. On the other hand, the high correlation coefficient (R2 = 0.9861) obtained for the PSO kinetic model as shown in Fig. 10(b), indicates that it provides a better fit for the experimental data. This suggests a strong interaction between MB molecules with the CCC, with chemisorption as one of the rate-controlling steps [46]. The low PSO rate constant (k2) indicates a rapid removal in the initial stage, followed by slower adsorption due to saturation of the active sites [47].

The Weber-Morris intraparticle diffusion model was used to analyze the adsorption kinetics of MB removal using CCC. This model is useful in determining the rate-limiting mechanism of MB removal by CCC. Table 7 provides the Weber-Morris constant, and Fig. 11 illustrates the plot of the adsorption kinetics based on the Weber-Morris model.

Table 7 *Webber Morris constant for MB removal using CCC*

Region	R^2	k_{id} (mg/g.min$^{1/2}$)	C (mg/g)
1	0.9696	0.7571	-0.03362
2	0.9329	0.4544	2.7574
3	0.1160	-0,0321	8.767

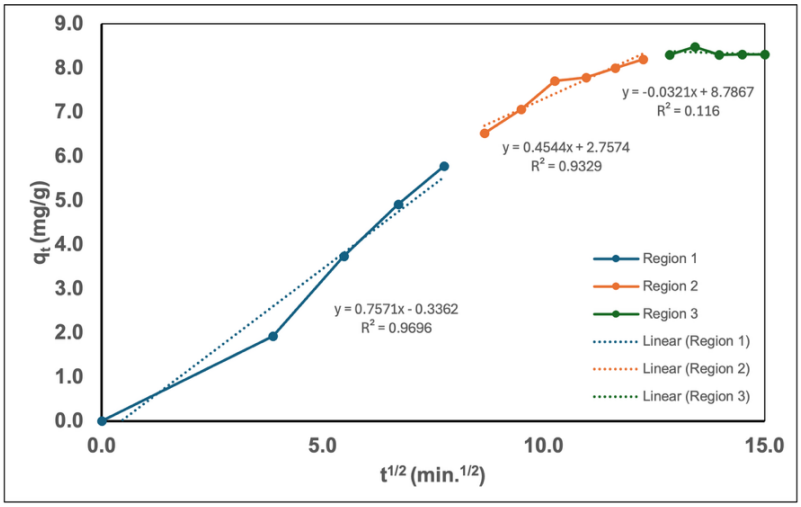

Fig. 11 *Weber–Morris intraparticle diffusion model for MB removal by CCC*

Based on Fig. 11, the adsorption of MB using CCC can be divided into three different regions. In the region I (0-75 min.), a high value of kid (0.7571 mg/g.$t^{1/2}$) indicates that MB removal occurred through a rapid surface adsorption and boundary layer diffusion. As the intercept (C = -0.3362 mg/g) doesn't pass through the origin, it shows that MB removal at this stage involves not only intraparticle diffusion but also surface adsorption. In region 2 (75-150 min.), a low k_{id} (k_{id} = 0.4544 mg/g.$t^{1/2}$), and a high intercept value (C = 2.7574 mg/g) suggest that MB molecules were adsorbed into the internal pores of CCC mainly through intraparticle diffusion, until the active sites on CCC became saturated. In region 3 (150-225 min.), an almost constant slope (k = -0.0321 mg/g.$min^{1/2}$) and very low correlation of coefficients (R^2 = 0.116) indicated the equilibrium has been reached, and intra-particle diffusion no longer plays a vital role in the adsorption process.

The findings from this study reveal that MB removal by CCC occurs through a multi-stage mechanism, which involves both internal diffusion and intraparticle diffusion; however, intraparticle diffusion is not the sole rate-limiting step.

4. Conclusions

In this paper, the performance of three different adsorbents was evaluated for the removal of methylene blue (MB) from the synthetic dye. Those adsorbents include commercial activated carbon (CAC), untreated confiscated cigarettes (CC), and chemically treated confiscated cigarettes (CCC). It was found that CAC outperforms both CC and CCC, with CCC performing better than CC. Although CCC is less superior than CAC, it is more sustainable and aligned with economic principles by converting waste from confiscated cigarettes into adsorbents. The characterization study by SEM reveals the enhancement of pore formation in the CCC, while FTIR analysis indicates the formation of carboxylic acid groups, which contribute to the removal of MB. From the adsorption isotherm study, it was found that MB removal by using CCC better fits the Langmuir isotherm model, which implies a monolayer adsorption.

Additionally, kinetic analysis indicated that the PSO more accurately represents the experimental data, with a high correlation coefficient of 0.9861, indicating that the mechanisms involve chemisorption. Further analysis using the Weber-Morris model reveals that intra-particle diffusion also affects the MB removal by CCC. Based on the findings of this study, further research should be conducted on optimizing adsorbent preparation methods, regenerating spent adsorbents, and their scalability.

Acknowledgement

The authors thank the Malaysian Ministry of Higher Education for funds approved under '*MTUN Sepadan 2023*' (9032-00012).

Conflict of Interest

The authors declare no conflict of interest regarding the publication of this paper.

Author Contribution

The authors confirm their contributions to the paper as follows: ***study conception and design:*** *Saiful Azhar Saad, Khairuddin Md Isa, Subash Candra Bose Gopinath;* ***data collection:*** *Saiful Azhar Saad;* ***analysis and interpretation of results****: Naimah Ibrahim, Farizul Hafiz Kasim;* ***draft manuscript preparation:*** *Saiful Azhar Saad, Mohd Aizudin Abd Aziz. All authors reviewed the results and approved the final version of the manuscript.*

References

[1] Xiao, W., Garba, Z. N., Sun, S., Lawan, I., Wang, L., Lin, M. & Yuan, Z. (2020) Preparation and evaluation of an effective activated carbon from white sugar for the adsorption of rhodamine B dye, *Journal of Cleaner Production, 253*, 119989, https://doi.org/10.1016/j.jclepro.2020.119989

[2] Al-Tohamy, R., Ali, S. S., Li, F., Okasha, K. M., Mahmoud, Y. A. G., Elsamahy, T., Jiao, H., Fu, Y. & Sun, J. (2022) A critical review on the treatment of dye-containing wastewater: Ecotoxicological and health concerns of textile dyes and possible remediation approaches for environmental safety, *Ecotoxicology and Environmental Safety, 231*, 113160, https://doi.org/10.1016/j.ecoenv.2021.113160

[3] Robinson, T., McMullan, G., Marchant, R. & Nigam, P. (2001). Remediation of dyes in textile effluent: a critical review on current treatment technologies with a proposed alternative, *Bioresource Technology, 77*, 247-255, https://doi.org/10.1016/S0960-8524(00)00080-8

[4] Haleem, A., Shafiq, A., Chen, S. -Q. & Nazar, M. *A Comprehensive Review on Adsorption, Photocatalytic and Chemical Degradation of Dyes and Nitro-Compounds over Different Kinds of Porous and Composite Materials*. Molecules, 2023. **28**, DOI: 10.3390/molecules28031081.

[5] Lellis, B., Fávaro-Polonio, C. Z., Pamphile, J. A. & Polonio, J. C. (2019). Effects of textile dyes on health and the environment and bioremediation potential of living organisms, *Biotechnology Research and Innovation, 3*, 275-290, https://doi.org/10.1016/j.biori.2019.09.001

[6] Samsami, S., Mohamadizaniani, M., Sarrafzadeh, M. -H., Rene, E. R. & Firoozbahr, M. (2020). Recent advances in the treatment of dye-containing wastewater from textile industries: Overview and perspectives, *Process Safety and Environmental Protection, 143*, 138-163, https://doi.org/10.1016/j.psep.2020.05.034

[7] Valli Nachiyar, C., Rakshi, A.D., Sandhya, S., Britlin Deva Jebasta, N. & Nellore, J. (2023). Developments in treatment technologies of dye-containing effluent: A review, *Case Studies in Chemical and Environmental Engineering, 7*, 100339, https://doi.org/10.1016/j.cscee.2023.100339

[8] Vieira, A. P., Santana, S. A. A., Bezerra, C. W. B., Silva, H. A. S., Chaves, J. A. P., de Melo, J. C. P., da Silva Filho, E. C. & Airoldi, C. (2009). Kinetics and thermodynamics of textile dye adsorption from aqueous solutions using babassu coconut mesocarp, *Journal of Hazardous Materials, 166*, 1272-1278, https://doi.org/10.1016/j.jhazmat.2008.12.043

[9] Dehmani, Y., Franco, D. S. P., Georgin, J., Mghaiouini, R., Mohammed, B. B., Kacimi, R., Lamhasni, T., Lima, E. C., El Messaoudi, N. & Sadik, A. (2025). Towards a deeper understanding of the adsorption of methyl orange on a commercial activated carbon: Study of impact factors, isotherm and mechanism, *Environmental Surfaces and Interfaces, 3*, 103-111, https://doi.org/10.1016/j.esi.2025.02.002

[10] Kannan, N. & Sundaram, M. M. (2001). Kinetics and mechanism of removal of methylene blue by adsorption on various carbons-a comparative study, *Dyes and Pigments, 51*, 25-40, https://doi.org/10.1016/S0143-7208(01)00056-0

[11] Rafatullah, M., Sulaiman, O., Hashim, R. & Ahmad, A. (2010). Adsorption of methylene blue on low-cost adsorbents: A review, *Journal of Hazardous Materials, 177*, 70-80, https://doi.org/10.1016/j.jhazmat.2009.12.047

[12] Saad, S. A., Isa, K.M. & Bahari, R. (2010). Chemically modified sugarcane bagasse as a potentially low-cost biosorbent for dye removal, *Desalination, 264*, 123-128, https://doi.org/10.1016/j.desal.2010.07.015

[13] Ihaddaden, S., Aberkane, D., Boukerroui, A. & Robert, D. (2022). Removal of methylene blue (basic dye) by coagulation-flocculation with biomaterials (bentonite and Opuntia ficus indica), *Journal of Water Process Engineering, 49*, 102952, https://doi.org/10.1016/j.jwpe.2022.102952

[14] Zourif, A., Kouniba, S. & El Guendouzi, M. (2025). Valorization of palm petiole waste as natural biocoagulants: Optimizing coagulation-flocculation for sustainable wastewater treatment and advancing circular economy in agriculture, *Biocatalysis and Agricultural Biotechnology, 63*, 103473, https://doi.org/10.1016/j.bcab.2024.103473

[15] Rivera, F. L., Recio, F. J., Palomares, F. J., Sánchez-Marcos, J., Menéndez, N., Mazarío, E. & Herrasti, P. (2020). Fenton-like degradation enhancement of methylene blue dye with magnetic heating induction*, Journal of Electroanalytical Chemistry, 879*, 114773, https://doi.org/10.1016/j.jelechem.2020.114773

[16] Ghauch, A., Tuqan, A. M., Kibbi, N. & Geryes, S. (2012). Methylene blue discoloration by heated persulfate in aqueous solution*, Chemical Engineering Journal, 213*, 259-271, https://doi.org/10.1016/j.cej.2012.09.122

[17] Soo, X. Y. D., Lee, J. J. C., Wu, W.-Y., Tao, L., Wang, C., Zhu, Q. & Bu, J. (2024). Advancements in CO2 capture by absorption and adsorption: A comprehensive review*, Journal of CO2 Utilization, 81*, 102727, https://doi.org/10.1016/j.jcou.2024.102727

[18] Hab Alrman, K., Alhariri, S. & Al- Bakri, I. (2024). Ultrafiltration membrane based on chitosan/adipic acid: Synthesis, characterization and performance on separation of methylene blue and reactive yellow-145 from aqueous phase*, Heliyon, 10*, e31055, https://doi.org/10.1016/j.heliyon.2024.e31055

[19] Alatabe, M. J. A. & Ghorbanpour, M. (2024). A performance comparison of photo-fenton decolorization of methylene blue by using bentonite/iron composites prepared by liquid phase and solid phase ion exchange method*, Desalination and Water Treatment, 317*, 100027, https://doi.org/10.1016/j.dwt.2024.100027

[20] Jafarpisheh, F. & Ghorbanpour, M. (2023). Photocatalytic decolorization of Methylene Blue by using solid-state zinc exchanged clinoptilolite*, Desalination and Water Treatment, 289*, 221-227, https://doi.org/10.5004/dwt.2023.29411

[21] Yeo, T. H. C., Tan, I. A. W. & Abdullah, M. O. (2012). Development of adsorption air-conditioning technology using modified activated carbon – A review*, Renewable and Sustainable Energy Reviews, 16*, 3355-3363, https://doi.org/10.1016/j.rser.2012.02.073

[22] Kurniasih, M., Aprilita, N. H., Roto, R. & Mudasir, M. (2025). Modification of coal fly ash for high capacity adsorption of methylene blue*, Case Studies in Chemical and Environmental Engineering, 11*, 101101, https://doi.org/10.1016/j.cscee.2025.101101

[23] Bharathi, K. S. & Ramesh, S. T. (2013). Removal of dyes using agricultural waste as low-cost adsorbents: a review*., Applied Water Science 3, 3*, 773-790, https://doi.org/10.1007/s13201-013-0117-y

[24] Koya, R. K., Branston, J. R. & Gallagher, A. W. A. (2022). Measuring Malaysia's Illicit Tobacco Trade: An Excise Tax Gap Analysis*, journal of Illicit Economies and Development, 4*, 58-70,

[25] Ahmed, M. J. & Hameed, B. H. (2024). Recent progress on tobacco wastes–derived adsorbents for the remediation of aquatic pollutants: A review*, Environmental Research, 247*, 118203, https://doi.org/10.1016/j.envres.2024.118203

[26] Manfrin, J., Gonçalves Jr, A. C., Schwantes, D., Conradi Jr, E., Zimmermann, J. & Ziemer, G. L. (2021). Development of biochar and activated carbon from cigarettes wastes and their applications in Pb2+ adsorption*, Journal of Environmental Chemical Engineering, 9*, 104980, https://doi.org/10.1016/j.jece.2020.104980

[27] Conradi, E., Gonçalves, A. C., Schwantes, D., Manfrin, J., Schiller, A., Zimmerman, J., Klassen, G. J. & Ziemer, G. L. (2019). Development of renewable adsorbent from cigarettes for lead removal from water*, Journal of Environmental Chemical Engineering, 7*, 103200, https://doi.org/10.1016/j.jece.2019.103200

[28] García-Rollán, M., Sanz-Santos, E., Belver, C. & Bedia, J. (2025). Key adsorbents and influencing factors in the adsorption of micro- and nanoplastics: A review*, Journal of Environmental Management, 383*, 125394, https://doi.org/10.1016/j.jenvman.2025.125394

[29] Aygün, A., Yenisoy-Karakaş, S. & Duman, I. (2003). Production of granular activated carbon from fruit stones and nutshells and evaluation of their physical, chemical and adsorption properties*, Microporous and Mesoporous Materials, 66*, 189-195, https://doi.org/10.1016/j.micromeso.2003.08.028

[30] Kavitha, D. & Namasivayam, C. (2007). Experimental and kinetic studies on methylene blue adsorption by coir pith carbon*, Bioresource Technology, 98*, 14-21, https://doi.org/10.1016/j.biortech.2005.12.008

[31] Wu, F. -C. & Tseng, R. -L. (2008). High adsorption capacity NaOH-activated carbon for dye removal from aqueous solution*, Journal of Hazardous Materials, 152*, 1256-1267, https://doi.org/10.1016/j.jhazmat.2007.07.109

[32] Tseng, R. -L., Tseng, S. -K. & Wu, F. -C. (2006). Preparation of high surface area carbons from Corncob with KOH etching plus CO2 gasification for the adsorption of dyes and phenols from water*, Colloids and Surfaces A: Physicochemical and Engineering Aspects, 279*, 69-78, https://doi.org/10.1016/j.colsurfa.2005.12.042

[33] De Gisi, S., Lofrano, G., Grassi, M. & Notarnicola, M. (2016). Characteristics and adsorption capacities of low-cost sorbents for wastewater treatment: A review*, Sustainable Materials and Technologies, 9*, 10-40, https://doi.org/10.1016/j.susmat.2016.06.002

[34] Heidarinejad, Z., Rahmanian, O., Fazlzadeh, M. & Heidari, M. (2018). Enhancement of methylene blue adsorption onto activated carbon prepared from Date Press Cake by low frequency ultrasound*, Journal of Molecular Liquids, 264*, 591-599, https://doi.org/10.1016/j.molliq.2018.05.100

[35] Munonde, T. S., Nqombolo, A., Hobongwana, S., Mpupa, A. & Nomngongo, P. N. (2023). Removal of methylene blue using MnO2@rGO nanocomposite from textile wastewater: Isotherms, kinetics and thermodynamics studies*, Heliyon, 9*, e15502, https://doi.org/10.1016/j.heliyon.2023.e15502

[36] Jihyun R. Kim, Branden Santiano, Hyosang Kim & Kan, E. (2013). Heterogeneous Oxidation of Methylene Blue with Surface-Modified Iron-Amended Activated Carbon*, American Journal of Analytical Chemistry, 4*, 115-122, 10.4236/ajac.2013.47A016.

[37] Lee, H., Fiore, S. & Berruti, F. (2024). Adsorption of methyl orange and methylene blue on activated biocarbon derived from birchwood pellets*, Biomass and Bioenergy, 191*, 107446, https://doi.org/10.1016/j.biombioe.2024.107446

[38] Malbenia John, M., Benettayeb, A., Belkacem, M., Ruvimbo Mitchel, C., Hadj Brahim, M., Benettayeb, I., Haddou, B., Al-Farraj, S., Alkahtane, A. A., Ghosh, S., Chia, C. H., Sillanpaa, M., Baigenzhenov, O. & Hosseini-Bandegharaei, A. (2024). An overview on the key advantages and limitations of batch and dynamic modes of biosorption of metal ions*, Chemosphere, 357*, 142051, https://doi.org/10.1016/j.chemosphere.2024.142051

[39] Kandil, H. & El-Wakeel, S. T. (2024). Kandil, H., El-Wakeel, S. T. Effective removal of Pb(II) and Cu(II) from aqueous solutions using a hybrid composite of fuller's earth, aluminum silicate and chitosan.*, Polym. Bull., 81*, 1839-1854, https://doi.org/10.1007/s00289-023-04792-8

[40] Gryglewicz, G., Machnikowski, J., Lorenc-Grabowska, E., Lota, G. & Frackowiak, E. (2005). Effect of pore size distribution of coal-based activated carbons on double layer capacitance*, Electrochimica Acta, 50*, 1197-1206, https://doi.org/10.1016/j.electacta.2004.07.045

[41] Arain, M. B. & Soylak, M. (2025). Layered triple hydroxide (NiCoFe-LTH) with g-C3N4 hybrid nanocomposite as an adsorbent for Pb(II) extraction*, Food Chemistry,* 142766, https://doi.org/10.1016/j.foodchem.2025.142766

[42] da Silva Bruckmann, F., da Rosa Salles, T., Knani, S., Graba, B., Baumann, L., Müller, E. I., Garcia, W. J. S., de Oliveira, A. H., Alves, M. d. C. M., Morais, J., da Boit Martinello, K., Silva, L. F. O., Dotto, G. L. & Rhoden, C. R. B. (2024). Removal of ivermectin from aqueous medium on chitosan-based magnetic adsorbent*, Inorganic Chemistry Communications, 169*, 113006, 10.1016/j.inoche.2024.113006

[43] Siddiqa, A., Khatun, M. H. & Mostafa, M. G. (2025). Synthesis of magnetite-maghemite nanocomposite adsorbents coated with leaf extract for removal of lead ions from water*, Desalination and Water Treatment, 321*, 100979, https://doi.org/10.1016/j.dwt.2024.100979

[44] Ashraf, B., Mubarak, S., Asghar, A., Hafeez, A. & Asif, F. (2025). Recycling fruit peels into :magnetite/carbon adsorbents: A scalable solution for pyrethroid insecticide removal*, Desalination and Water Treatment, 321*, 100884, https://doi.org/10.1016/j.dwt.2024.100884

[45] Kamal, W., Essam, D., Allam, A. A., Alfassam, H. E., abd el tawab, D., Moaty, S. A. & Mahmoud, R. (2025). Natural Egyptian zeolite ore as a novel layered adsorbent for petroleum wastewater treatment*, Chinese Journal of Analytical Chemistry,* 100490, https://doi.org/10.1016/j.cjac.2024.100490

[46] Chu, K. H., Bollinger, J.-C. & Kierczak, J. (2025). Pseudo-first-order kinetics in environmental adsorption: Why are there two distinct equations?*, Environmental Surfaces and Interfaces, 3*, 191-195, https://doi.org/10.1016/j.esi.2025.07.001

[47] Benjelloun, M., Miyah, Y., Akdemir Evrendilek, G., Zerrouq, F. & Lairini, S. (2021). Recent Advances in Adsorption Kinetic Models: Their Application to Dye Types*, Arabian Journal of Chemistry, 14*, 103031, https://doi.org/10.1016/j.arabjc.2021.103031